

Two-dimensional leaflet valves with maximum reverse-flow moment

E.O. TUCK

Department of Applied Mathematics, University of Adelaide, Adelaide, S.A.5001, Australia

(Received March 24, 1981)

SUMMARY

Camber and thickness distributions and a hinge point, are chosen for thin airfoils, to maximise the de-stabilising moment about that hinge point, in steady reversed flow. This optimisation is carried out subject to the constraints that the airfoil be in equilibrium for steady forward flow, and that the mean square camber be held fixed.

1. Introduction

A passive valve in the form of a thin leaflet, that almost aligns itself with the flow when open, has obvious advantages compared to (say) a ball in a cage. In the latter case, the ball remains as a major diverter of flow streamlines in the fully-open configuration. Such diversions are almost invariably undesirable.

It is not therefore surprising that nature has evolved leaflet-type valves for use in physiological systems, such as the cardio-vascular. Engineering design of passive valves, on the other hand, has tended to prefer ball types, mainly for reasons of simplicity. Even when man needed to replace nature's design by one of his own, as in prosthetic heart-valve replacements [1], the ball type was generally preferred, at first.

This preference was in part because of hinging difficulties, in part because of an apparent need for flexibility in the natural valve, and in part because of a need to keep the complete mechanism well washed. However, none of these difficulties is major, and some of the most successful recent prosthetic heart valve designs have involved rigid hinged cambered discs or leaflets [2].

It is immediately clear that some form of effective camber is desirable, if such a leaflet is to have the ability to close rapidly, while providing minimum obstruction to forward flow. That is, a rigid flat plate, fully aligned with a uniform stream, is of little or no use as a valve, since it will not have any immediate incentive to begin to re-align itself perpendicular to the stream, if the stream is reversed.

Admittedly, providing the plate is hinged at a point such that the forward-flow configuration is stable (ahead of quarter-chord, for a two-dimensional flow), the reverse flow will be unstable, and any small perturbation will cause the plate to depart from alignment. However, the designer can hardly rely on this instability mechanism, which is not certain as to direction, and would presumably be slow to begin.

More generally, the leaflet must, in the equilibrium fully-open configuration, present some

obstruction to a reversed flow, whether or not that flow is uniform. For example, the natural aortic valve leaflet is almost planar when fully open, but [3] the presence of “sinuses”, (i.e. small pockets in the aortic wall) guarantees that the reversed flow is locally non-uniform. This local flow non-uniformity is equivalent to a camber of the leaflet, in an otherwise-uniform undisturbed flow.

If our task is to design a rigid leaflet, we can easily introduce camber in the leaflet itself. Hence, in this paper, the task set is to choose an appropriate shape, in terms of camber and thickness, for the rigid leaflet, assuming that both the forward and reversed flows would be uniform in the absence of the leaflet.

This problem is treated as one in classical inviscid incompressible aerodynamics. That is, we assume that the Reynolds number of the flow is high enough that viscosity can be ignored, except in the sense that it determines, via a Kutta condition, the circulation around the leaflet. For the present, we also assume that the flow is two-dimensional; that is, that the aspect ratio of the leaflet is large. Although this is not really a good approximation for applications such as to the aortic valve, the extension to arbitrary aspect ratio, or to an axisymmetric flow, is straightforward in principle.

We also assume that both the forward and reversed flows are steady. This is not unreasonable for the forward flow, which any successful design ensure is smooth and steady. However, in the application to the aortic valve, an important feature [3] neglected by the assumption of steadiness is a tendency of the natural valve to commence closing as the forward decelerates. Although this feature is not included in the present theory [but see note on p. 57], it seems intuitively reasonable that designs optimised for steady flow will also have favourable ‘anticipatory’ properties, in decelerating forward flow.

For the reversed flow, even though our aim is to induce motion of the leaflet, we assume that sufficient time elapses from the commencement of reversed flow, for the required steady circulation to develop. This steady reversed flow (about the leaflet in its equilibrium forward-flow configuration) will exert unbalanced forces and moments on the leaflet, causing it to move, so creating flow unsteadiness and ultimately closing off the reversed flow. In spite of this ‘slowed-down’ description of events, we are in fact anxious to design a leaflet such that closure occurs as rapidly as possible.

The arguments advanced above in favour of camber clearly extend to the conclusion that maximum rate of closure will occur for a very highly cambered leaflet. Since this would defeat the purpose of the exercise, the leaflet being intended to be a small perturber of the forward flow, some form of constraint on camber is required, and we use a constraint on its mean-square value. In view of this limitation, the leaflet can be considered as a thin airfoil, and the classical theory of such airfoils [4] can be exploited.

The simplest problem of this sort to analyse, is that for an airfoil alone in an unbounded uniform stream. This analysis is presented in Sec. 2. The result is very simple, indicating that the optimal ‘valve’ is of zero thickness, has a camber that is large near the leading edge of the forward flow, reducing to zero at the trailing edge, and is hinged at a point 9% of chord from the leading edge.

Clearly, such a design is not much use as a valve, since it cannot block off the flow completely, when perpendicular to it. This situation can be remedied by introducing boundaries to the

undisturbed flow. The analysis is then repeated for the case when there is just one such boundary, an infinite plane wall, parallel to the undisturbed stream.

Now an analytic solution is not possible, and we must resort to numerical techniques. The problem of an airfoil moving in the neighbourhood of a plane wall has been solved numerically in other contexts (e.g. [5]), and we need merely adapt computer programs already developed for other purposes. The results show that the optimal leaflet not only is cambered, but also possesses thickness, and we find the optimal distribution of both these quantities, and the corresponding optimal hinge point.

Although this configuration is, by itself, still incapable of functioning as a true valve, such a valve can be constructed by incorporating a second boundary wall, or by combining two such leaflets symmetrically. In principle, it is necessary to analyse the combined flow; however, the optimal leaflet, when fully open, is sufficiently close to the original wall, to make it reasonable to assume that the second wall or leaflet has little effect. A suitable design for such a valve is provided, the hinge point being at 21% of chord from the leading edge of the forward flow.

2. Unbounded fluid

If a thin airfoil is alone in an unbounded fluid, its thickness does not influence the lift distribution on it. Hence, from the point of view of maximisation of rate of closure, leaflet thickness is irrelevant, and will be taken as zero in the present section. That is, the leaflet is taken to have equation

$$y = f(x), \quad |x| < \ell, \quad (2.1)$$

where 2ℓ is the chord. The derivative of the function $f(x)$ includes both of what are normally described as camber and angle-of-attack contributions, and is taken as a small quantity.

If this thin airfoil is placed in a uniform stream U in the x -direction, of fluid of density ρ , the pressure jump $\rho U \gamma(x)$ across the foil satisfies the integral equation ([4], p. 170)

$$\frac{1}{\pi} \int_{-\ell}^{\ell} \frac{\gamma(\xi)}{x - \xi} d\xi = 2Uf'(x). \quad (2.2)$$

According to the Kutta condition, the pressure jump must vanish at the trailing edge, namely $x = +\ell$ if $U > 0$, or at $x = -\ell$ if $U < 0$. The resulting explicit solution of (2.2) is then ($U \geq 0$)

$$\gamma^{\pm}(x) = -\frac{2U^2}{\pi} \sqrt{\frac{\ell \mp x}{\ell \pm x}} \int_{-\ell}^{\ell} \sqrt{\frac{\ell \pm \xi}{\ell \mp \xi}} \frac{f'(\xi)}{x - \xi} d\xi. \quad (2.3)$$

The corresponding moment about $x = x_0$ is

$$M^{\pm} = -\rho U \int_{-\ell}^{\ell} (x - x_0) \gamma^{\pm}(x) dx \quad (2.4)$$

$$= 2\rho U^2 \int_{-\ell}^{\ell} [\ell \pm (x_0 - x)] \sqrt{\frac{\ell \pm x}{\ell \mp x}} f'(x) dx. \quad (2.5)$$

Our task is to choose the shape function $f'(x)$ and hinge position x_0 , so as to maximise M^- , while $M^+ = 0$. That is, we maximise the overturning moment about x_0 in reversed flow, given that the configuration is originally in equilibrium for forward flow. At the same time, we must place a bound on the size of $f'(x)$, since it is immediately clear that M^- can be increased without bound by letting $f' \rightarrow \infty$.

For that purpose, we use the quantity

$$E = \int_{-\ell}^{\ell} f'(x)^2 dx. \quad (2.6)$$

This can either be interpreted as the 'mean square camber', or as an approximation to the excess of arc length over chord. In any case, reducing E tends to reduce the extent to which the leaflet disturbs the forward flow.

Now the task of maximising M^- subject to the constraint that E is fixed, is an elementary one in the calculus of variations [6], with the solution

$$f'(x) = \lambda(\ell - x_0 + x) \sqrt{\frac{\ell - x}{\ell + x}}, \quad (2.7)$$

for some Lagrange multiplier λ . The resulting value of M^+ is

$$M^+ = 4\rho U^2 \lambda \ell \left[\frac{2}{3} \ell^2 - x_0^2 \right] \quad (2.8)$$

which vanishes if

$$x_0^2 = \frac{2}{3} \ell^2 \quad (2.9)$$

e.g. at $x_0 = -0.8165\ell$. This particular choice of x_0 is stable for the forward flow, since it is forward of the centre of pressure, $x = -\frac{1}{2}\ell$. The shape of the optimum leaflet is shown in Figure 1, as the curve $h = \infty$.

The corresponding linear-theory values of M^- and E are in fact logarithmically positive infinite. However, this singularity does not invalidate the variational procedure, the choices (2.7) and (2.9) being preferable over all other camber and hinge positions, irrespective of convergence of the resulting integrals. Obviously we are not unhappy about a large positive value for M^- , but we had hoped to keep E bounded.

Inclusion of non-linear effects near the highly cambered leading edge $x = -\ell$, provides a remedy for this difficulty. It is possible to see how this will occur, even using the linearized solution, if we exclude a small neighbourhood of $x = -\ell$ from the integrals in (2.5) and (2.6). But then the integrals for M^- and E are proportional to each other, and we have

$$M^- = \frac{2\rho U^2}{\lambda} E. \quad (2.10)$$

That is, as we reduce the scale λ of the camber function $f'(x)$, keeping E fixed, M^- will become larger and larger, as required.

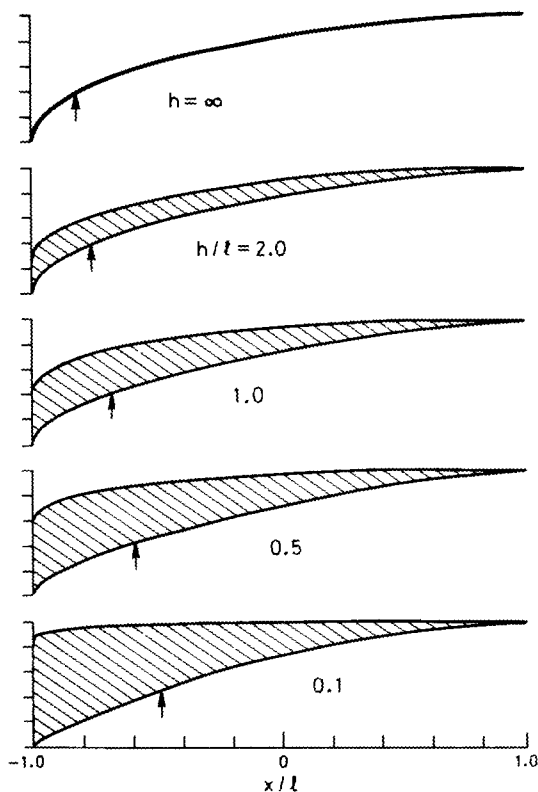


Figure 1. Optimal valve shapes. Arrows show optimal hinge points.

3. Leaflet near a plane wall

If a thin airfoil is placed at $y = h$ in a steady flow near a wall $y = 0$, the flow is the same as if there was a mirror-image foil at $y = -h$. The local flow, as seen by the original foil, is now influenced by the image foil, and in particular, an additional effective camber is induced by that image's thickness. Hence, we can no longer treat the leaflet as one of zero thickness.

Suppose, therefore, that the foil has upper and lower surfaces.

$$y = h + f_{\pm}(x), \quad |x| < \ell, \quad (3.1)$$

respectively. Then, in a stream U , the perturbation velocity potential ϕ satisfies the linearized boundary condition ([4], p. 165)

$$\phi_y(x, h \pm 0) = Uf'_{\pm}(x), \quad |x| < \ell. \quad (3.2)$$

The velocity potential ϕ must vanish at infinity, satisfy Laplace's equation everywhere, and $\phi_y = 0$ on $y = 0$. A suitable representation of such a potential is (c.f. [7])

$$\phi(x, y) = \int_{-\ell}^{\ell} [q(\xi)G(x - \xi, y) + \gamma(\xi)H(x - \xi, y)] d\xi \quad (3.3)$$

where

$$G(x, y) = \frac{1}{4\pi} \log [(x^2 + (y - h)^2)(x^2 + (y + h)^2)] \quad (3.4)$$

and

$$H(x, y) = \frac{1}{2\pi} \arctan \frac{y - h}{x} - \frac{1}{2\pi} \arctan \frac{y + h}{x}. \quad (3.5)$$

The expression (3.3) is just a distribution of sources of strength q , and vortices of strength γ , together with their images in $y = 0$.

Now, upon application of the boundary conditions (3.2) as $y \rightarrow h \pm 0$, we find

$$\begin{aligned} \pm \frac{1}{2} q(x) + \frac{h}{\pi} \int_{-\ell}^{\ell} \frac{q(\xi) d\xi}{(x - \xi)^2 + 4h^2} + \frac{1}{2\pi} \int_{-\ell}^{\ell} d\xi \gamma(\xi) \left[\frac{1}{x - \xi} - \frac{x - \xi}{(x - \xi)^2 + 4h^2} \right] \\ = U f'_{\pm}(x). \end{aligned} \quad (3.6)$$

That is, the source strength $q(x)$ is determined explicitly as

$$q(x) = 2U g'(x) \quad (3.7)$$

where

$$2g(x) = f_+(x) - f_-(x) \quad (3.8)$$

is the thickness of the leaflet.

On the other hand, the vortex strength $\gamma(x)$ satisfies the integral equation

$$\frac{1}{\pi} \int_{-\ell}^{\ell} d\xi \gamma(\xi) \left[\frac{1}{x - \xi} - \frac{x - \xi}{(x - \xi)^2 + 4h^2} \right] = 2U (f'(x) + f'_I(x)) \quad (3.9)$$

where

$$f(x) = \frac{1}{2} [f_+(x) + f_-(x)] \quad (3.10)$$

defines the mean surface of the leaflet, i.e. $f'(x)$ is its camber, and

$$f'_I(x) = - \frac{2h}{\pi} \int_{-\ell}^{\ell} \frac{g'(\xi) d\xi}{(x - \xi)^2 + 4h^2} \quad (3.11)$$

is the additional induced camber due to image thickness.

Equation (3.9) is the generalization of (2.2). In fact, as $h \rightarrow \infty$, $f'_I(x) \rightarrow 0$; i.e. the effect of thickness vanishes in this limit, as expected. At the same time, the kernel of the integral equation (3.9) reduces to that of (2.2). However, (3.9) possesses no explicit analytic solution like (2.3), and we must resort to numerical methods.

The generalization of the mean camber constraint (2.6) is

$$E = \frac{1}{2} \int_{-\ell}^{\ell} [f'_+(x)^2 + f'_-(x)^2] dx \quad (3.12)$$

$$= \int_{-\ell}^{\ell} [f'(x)^2 + g'(x)^2] dx. \quad (3.13)$$

This measures (according to (3.12)) the excess arc length of both top and bottom surfaces, or, according to (3.13), the mean square of both camber and thickness. Again, a reduction in E , implies a reduction in forward flow impediment.

The problem of maximising M^- subject to fixed E , now has two independent functions f' and g' to vary, and is not quite as trivial an exercise in the calculus of variations as that in Sec. 2. In addition, the lack of an explicit expression such as (2.5) for the moment M^- , in terms of the varying functions, makes our task difficult. The result of enforcing stationarity of $E + \lambda M^-$ is a set of integral relations of the form

$$\frac{1}{\pi} \int_{-\ell}^{\ell} d\xi f'(\xi) \left[\frac{1}{x - \xi} - \frac{x - \xi}{(x - \xi)^2 + 4h^2} \right] = \lambda(x - x_0) \quad (3.14)$$

and

$$g'(x) = - \frac{2h}{\pi} \int_{-\ell}^{\ell} d\xi \frac{f'(\xi)}{(x - \xi)^2 + 4h^2}. \quad (3.15)$$

Equation (3.14) must be solved subject to $f'(\ell) = 0$. It should be noted that (2.7) is the analytic solution of (2.2), subject to this condition.

Once $f'(x)$ is determined by solving (3.14), the thickness slope $g'(x)$ follows from (3.15), and hence the induced camber $f'_I(x)$ from (3.11). Finally, we must solve (3.9) for $\gamma = \gamma^+(x)$, satisfying $\gamma(\ell) = 0$, and choose the hinge point x_0 so that $M^+ = 0$.

As well as the limit $h \rightarrow \infty$, in which the theory of the present section reduces to that of Sec. 2, it is also possible to obtain analytic results as $h \rightarrow 0$, i.e. for very small gaps between leaflet and wall. In the first place, as $h \rightarrow 0$, equation (3.15) indicates that

$$g'(x) \rightarrow -f'(x). \quad (3.16)$$

That is, $f'_+(x) \rightarrow 0$, and the upper surface of the leaflet becomes plane. This allows the flow through the small gap to control the dynamics. At the same time, (3.14) yields

$$f''(x) = - \frac{\lambda}{2h} (x - x_0) \quad (3.17)$$

which may be integrated to give a cubic expression for the mean surface, and hence for the lower surface $f_-(x)$. The resulting optimum hinge point has $x_0^2 = \frac{1}{5}\ell^2$, i.e. $x_0 \simeq -0.45\ell$. These small $-h$ limiting results can also be obtained directly, using the small-gap theory of airfoils in ground effect (e.g. [8]).

4. Numerical solution

Our first need is for a computational procedure to solve the integral equation

$$\int_{-\ell}^{\ell} d\xi \gamma(\xi) K(x - \xi) = R(x) \quad (4.1)$$

where

$$K(x) = \frac{1}{x} - \frac{x}{x^2 + 4h^2}, \quad (4.2)$$

for various right-hand-side functions $R(x)$, subject to $\gamma(\ell) = 0$. A variety of techniques were discussed in [9], and Oertel's method [10] was found to work well in the present case. The resulting algorithm gives an output set of N values of $\gamma(x)$, for any set of N input values of $R(x)$, after inversion of a suitable $N \times N$ matrix. The errors tend to zero at least as fast as N^{-2} , and are less than $\frac{1}{2}\%$ for $N \geq 30$.

For example, if $R(x)$ is a constant, the output is the pressure distribution on a rigid flat plate at a constant angle of attack, at a distance h from a plane wall. From this pressure distribution, we may compute the centre of pressure for forward flow, shown as the dashed line in Figure 2. Similar results have been obtained by Hess [5] and others. This quantity is of importance in the present case, since any hinge point must be forward of the centre of pressure, to guarantee stability of the forward flow.

In order to solve (3.14) for the optimum leaflet shape, we first solve two canonical problems, for $\gamma = f_1'$ with $R = 1$, and for $\gamma = f_2'$ with $R = x$. Thus, the true camber is a linear combination of the form

$$f'(x) = \lambda [f_2'(x) - x_0 f_1'(x)]. \quad (4.3)$$

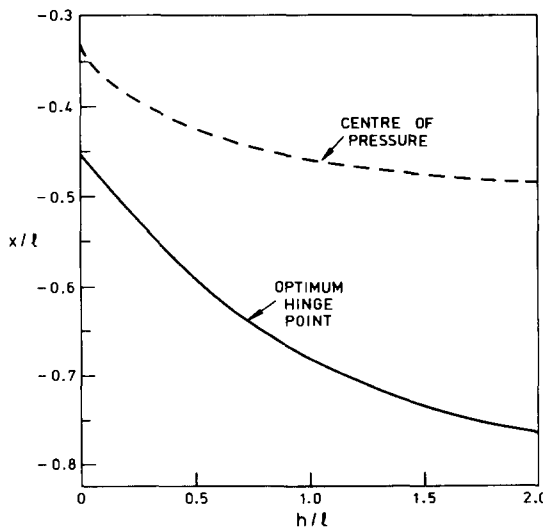


Figure 2. Variation in centre of pressure and optimal hinge point x_0 with distance h from wall.

However, the hinge point x_0 is so far not known, and we must proceed to satisfy forward-flow equilibrium, in order to determine x_0 .

Straightforward numerical approximation of (3.15) yields the thickness distribution g' , as a similar linear combination, and repeating this process on the identical integral (3.11) yields the induced camber f'_I . Finally, the integral equation (3.9) is of the form (4.1), with R as a linear expression in x_0 and can be solved to yield

$$\gamma(x) = \gamma_2(x) + x_0 \gamma_1(x). \quad (4.4)$$

That is, $\gamma_1(x)$ is the result of carrying out the above sequence of computations starting with the original $R = 1$, and $\gamma_2(x)$ starting with $R = x$. Note that 4 separate inversions of the integral equation (4.1) are needed to complete this process.

The moment about x_0 can now be expressed (using (2.4)) as a quadratic expression in x_0 , of the form

$$M^+ = M_{22} - (M_{12} + M_{21})x_0 + M_{11}x_0^2 \quad (4.5)$$

where M_{11} and M_{12} are respectively the force and moment corresponding to $R = 1$, and M_{21} and M_{22} those corresponding to $R = x$. However, a fundamental symmetry theorem (c.f. [4], p. 296) guarantees that

$$M_{12} + M_{21} = 0. \quad (4.6)$$

That is, $M^+ = 0$ if

$$x_0^2 = -M_{22}/M_{11}. \quad (4.7)$$

The numerical results do not obey (4.6) exactly for all N , but converge to it rapidly as $N \rightarrow \infty$. The coefficients M_{11} and M_{22} are positive and negative respectively, and the negative solution of the quadratic equation (4.5) converges rapidly to the results shown as the solid line on Figure 2. Since this line lies beneath the dashed line for all h , the resulting predicted hinge point x_0 is stable for the forward flow.

Figure 1 shows a corresponding set of design shapes for the leaflet. The maximum departure from $y = 0$ is arbitrary, and has been scaled to unity. Note how the thickness tends to zero as $h \rightarrow \infty$, relative to this unit maximum camber, and the results agree with (2.7). At the other end of the scale, as $h \rightarrow 0$, the upper surface becomes flat, as predicted by (3.16), and the optimum leaflet has comparable thickness and camber.

5. A design valve

No attempt has so far been made to predict a 'best' value of the wall clearance h . The optimisation was carried out at fixed h , and all we have done is to find the best leaflet at that h , by maximising the moment M^- . It is important to note that M^- is *not* an appropriate objective func-

tion for a global optimisation, in which h is allowed to vary. In that case, we must also pay attention to the added moment of inertia of the valve.

That is, the real objective is to maximise the initial angular acceleration of the leaflet about x_0 . There is little point in producing a large value of M^- , if at the same time one creates a situation in which the valve is very reluctant to move, in spite of that moment. However, for thin leaflets, the moment of inertia is independent of camber and thickness, being the same as that of a flat plate at a uniform distance h from the wall. Thus, for a given h , the moment of inertia is constant, and optimisation proceeds by maximising the moment M^- .

It should be noted in passing, however, that the moment of inertia increases dramatically, as h decreases. That is, when we place a nearly-flat rigid leaflet close to a wall, it must become very reluctant to rotate itself away from that wall, due to the large inertia of the fluid that has to rush into the increasing gap. Hence, it seems likely that presence of a wall is a negative factor in this type of design, and that the best valve will have the largest h possible.

However, as indicated in Sec. 3, a finite value of h seems essential, if the valve is actually to be able to close. In fact, complete closure of the flow near the wall in the present single-wall geometry demands that

$$h = \ell + x_0. \quad (5.1)$$

If the predicted optimum x_0 is used, (5.1) demands $h = 0.43\ell$ and $x_0 = -0.57\ell$.

The design with these parameters is shown in Figure 3. This Figure shows a second wall at $y = \ell$, and a stop to enable the valve to remain closed. The forward flow in this channel should really be analysed afresh, since, in principle, the new wall at $y = \ell$ will change flow conditions from those assumed in the analysis of Sec. 3, which assumes that there is only one wall, at $y = 0$. However, the new wall is sufficiently far from the leaflet in its fully-open position, to suggest that any corrections will be small. A symmetrical two-leaflet design can also be constructed by mirror reflection of Figure 3.

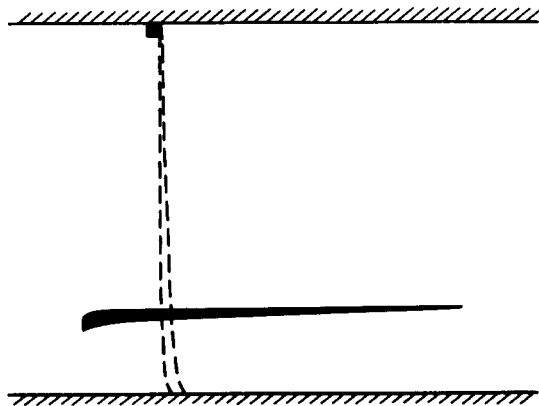


Figure 3. Example of a valve design. The solid outline is fully open, the dashed outline is fully closed.

6. Acknowledgements

Discussions with Dr. A. Helfgott of the Flinders Medical Centre, S.A., with Professors J. N. Newman and R. W. Yeung of M.I.T., and with Mr. T. Hearn are gratefully acknowledged. All computations were performed on a TRS-80 micro-computer.

REFERENCES

- [1] H. M. Windsor, M. X. Shanahan and V. P. Chang, Cardiac valve replacement, 1963-1979, *The Medical Journal of Australia* (1979) 53-56.
- [2] L. N. Scotten, R. G. Racca, A. N. Nugent, D. K. Walker, and R. T. Brownlee, The new tilting-disc cardiac valve prostheses. In vitro comparison of their hydrodynamic performance in the mitral position, *J. Thoracic Cardiovascular Surgery* (submitted 1980).
- [3] B. J. Bellhouse and L. Talbot, The fluid mechanics of the aortic valve, *J. Fluid Mech.* 35 (1969) 721-735.
- [4] J. N. Newman, *Marine hydrodynamics*, M.I.T. Press, Cambridge, Massachusetts, 1977.
- [5] F. Hess, Bank suction cancelled by rudder deflection: a theoretical model, *Int. Shipb. Prog.*, 25 (1978) 7-13.
- [6] J. W. Craggs, *Calculus of variations*, George Allen and Unwin, London, 1973.
- [7] E. O. Tuck, Some classical water-wave problems in varying depth, in: *Waves in water of varying depth*, ed. D. G. Provis and R. Radok, Springer-Verlag, Berlin, 1976.
- [8] E. O. Tuck, A non-linear unsteady one-dimensional theory for wings in extreme ground effect, *J. Fluid Mech.* 98 (1980) 33-47.
- [9] E. O. Tuck, Application and solution of Cauchy singular integral equations, in: *The application and numerical solution of integral equations*, ed. R. S. Anderssen et al., Sijthoff and Noordhoff, The Netherlands, 1980.
- [10] R. S. Oertel, *The steady motion of a flat ship, including an investigation of local flow near the bow*, Ph. D. thesis, University of Adelaide, 1975.

Note: Unsteady effects have now been included in a further study, University of Adelaide, Applied Mathematics Report T8106, July 1981.